Article

Not peer-reviewed version

Dose-Dependent Osteoinduction by rhBMP-2-Loaded β-Tricalcium Phosphate Scaffolds in Rabbit Critical-Sized Calvarial Defects: Histological, Histomorphometric, CD31 Immunohistochemical Evaluation

Solaf Abdulqadir Mustafa *, Chenar Anwar Mohammad, Rafal Abdulrazaq Alrawi

Posted Date: 23 March 2026

doi: 10.20944/preprints202603.1773.v1

Keywords: β-tricalcium phosphate; bone morphogenetic protein-2; critical size defect; immunohistochemistry; rabbit calvaria; osteogenesis

 doi:10.20944/preprints202603.1773.v1

Article

Dose-Dependent Osteoinduction by rhBMP-2-Loaded β-Tricalcium Phosphate Scaffolds in Rabbit Critical-Sized Calvarial Defects: Histological, Histomorphometric, CD31 Immunohistochemical Evaluation

Solaf Abdulqadir Mustafa [1,*], Chenar Anwar Mohammad [1] and Rafal Abdulrazaq Alrawi [2]

[1] Department of Periodontics, College of Dentistry, Hawler Medical University, Erbil 44001, Iraq

[2] Department of Clinical Analysis, College of Pharmacy, Hawler Medical University, Erbil 44001, Iraq

* Correspondence: solav.abdulqadir@hmu.edu.krd; Tel: +964 750 488 6537

Abstract

Critical-sized bone defects represent a major clinical challenge, as bone gaps of this magnitude are unable to heal spontaneously without regenerative intervention. The present study aimed to evaluate the dose-dependent osteoinductive effect of rhBMP-2–loaded β-TCP scaffolds on bone regeneration in critical-sized calvarial defects in a rabbit model. Eighteen adult male New Zealand White rabbits were used, and four circular defects (5 mm in diameter) were surgically created in the calvaria of each animal, resulting in a total of 72 defects. The animals were divided into four groups: control, β-TCP + 5 μg rhBMP-2, β-TCP + 10 μg rhBMP-2, and β-TCP + 20 μg rhBMP-2. Bone healing was evaluated at 2, 4, and 8 weeks postoperatively using histological and histomorphometric analyses. Masson's trichrome staining was performed to assess collagen deposition and maturation, while CD31 immunohistochemical staining was used to evaluate vascularization. The results demonstrated rhBMP-2–loaded β-TCP scaffolds significantly enhanced bone regeneration in a dose-dependent manner, with the β-TCP + 20 μg rhBMP-2 group demonstrating the greatest new bone formation and more mature bone architecture. In addition, BMP-2 treatment promoted osteoblastic activity, improved collagen maturation, and increased vascularization within the defect area. These findings indicate that rhBMP-2–loaded β-TCP scaffolds enhance bone regeneration in a dose-dependent manner, with higher rhBMP-2 doses resulting in greater bone formation and more mature bone architecture.

Keywords: β-tricalcium phosphate; bone morphogenetic protein-2; critical size defect; immunohistochemistry; rabbit calvaria; osteogenesis

1. Introduction

The dimension of a bone defect is a key determinant influencing its intrinsic regenerative capacity. When a defect surpasses a certain threshold—defined as a critical-sized defect—spontaneous bone healing fails to occur without the intervention of regenerative materials. In such circumstances, where osteoconductive matrices and osteogenic signals are insufficient, bone repair requires the incorporation of bioactive and osteoinductive agents to restore both structure and function (1).

Autografts continue to represent the standard grafting option, offering both structural support and biological stimulation for bone regeneration (2). Donor-site morbidity, limited supply, and the need for an additional surgery motivate the search for synthetic, bioactive alternatives (3). Consequently, calcium-phosphate bioceramics have attracted extensive interest because of their biocompatibility, predictable resorption, and ability to interact with cells and growth factors (4).

 doi:10.20944/preprints202603.1773.v1

Among the various synthetic bioceramics, β-tricalcium phosphate (β-TCP) has attracted particular attention for its proven safety and bone affinity. Its chemical composition and microstructure closely resemble those of natural bone, providing excellent osteoconductivity and biocompatibility, while its controlled biodegradation allows progressive substitution by newly formed bone (5). Nevertheless, β-TCP sometimes resorbs more rapidly than bone is deposited, producing an imbalance between scaffold loss and tissue regeneration (5).

Although some studies described an inherent osteoinductive capacity of β-TCP, this characteristic remains controversial and appears to vary across animal models, largely depending on the host's biological environment and circulating growth factors. These limitations have restricted the overall regenerative potential of β-TCP, prompting researchers to enhance its biological functionality by combining it with proteins, drugs, or growth factors (6).

Recombinant human bone morphogenetic protein-2 (rhBMP-2) is widely recognized as a key osteoinductive factor that has been extensively investigated for clinical use. BMPs belong to the transforming growth factor-β (TGF-β) superfamily and were first identified by Urist (7), who observed ectopic bone formation after implantation of demineralized bone matrix (8). Structurally, BMPs are dimeric proteins of approximately 120 amino acids stabilized by disulfide linkages and containing a heparin-binding region (9). Functionally, they govern cell proliferation, differentiation, matrix synthesis, and apoptosis. BMP-2 specifically promotes mesenchymal-stem-cell commitment to the osteoblastic lineage, stimulates osteoid deposition, and is clinically approved for use with collagen carriers in orthopedic and dental procedures (8).

Within critical-sized bone defects, BMP-2 serves a central regulatory role in coordinating osteogenesis and angiogenesis while modulating osteoclast activity through the Receptor Activator of Nuclear Factor Kappa-B Ligand (RANKL) pathway (10). Experimental studies have shown that bone formation rises proportionally with BMP-2 dose until an optimal level is reached, beyond which the response plateaus or declines (10).

The present study aimed to evaluate the effect of different doses of rhBMP-2 loaded β-TCP scaffolds on bone regeneration in critical-sized calvarial defects in a rabbit model. This research is driven by the need to optimize the BMP-2 dose that maximizes the osteoinductive efficiency of β-TCP while minimizing potential adverse effects. The findings are expected to provide useful information for developing safer and more efficient regenerative strategies relevant to clinical dentistry and orthopedic bone restoration.

2. Materials and Methods

2.1. Animal Model and Experimental Design

Upon approval of the study protocol by the Ethics Committee of Hawler Medical University, an in vivo experimental study was conducted at Hawler Medical University within the Central Animal Care Facility of the College of Pharmacy, Erbil, Kurdistan Region, Iraq. Eighteen healthy adult male New Zealand White rabbits, aged 12–16 weeks and weighing approximately 2.5–3.0 kg, were used in the study. Prior to surgery, all animals were acclimatized for one week under controlled laboratory conditions to minimize environmental stress and maintain physiological stability. Under general anesthesia, four standardized circular full-thickness defects, each measuring 5 mm in diameter, were created in the calvarial bone of each rabbit, with two defects on each side of the calvaria, resulting in a total of 72 defects. The four defects in each animal were randomly assigned to the experimental groups: control (left unfilled), β-TCP + 5 μg rhBMP-2, β-TCP + 10 μg rhBMP-2, and β-TCP + 20 μg rhBMP-2, as illustrated in Figure 2.

Synthetic β-tricalcium phosphate (adbone® TCP, Medbone® BioMaterials, Portugal), composed of 100% pure β-tricalcium phosphate, was used as the osteoconductive scaffold material. The material consisted of granules measuring 1–2 mm in diameter with approximately 80% interconnected porosity and a compressive strength of approximately 3 MPa.

 doi:10.20944/preprints202603.1773.v1

Recombinant human bone morphogenetic protein-2 (rhBMP-2; Elabscience Biotechnology Inc., Wuhan, China) was supplied in lyophilized form (100 μg/vial; purity >95%) and reconstituted with 0.5 mL sterile water for injection to yield a stock concentration of 200 μg/mL. After complete dissolution, aliquots of the stock solution were applied dropwise onto 0.1 g of β-TCP granules to obtain final doses of 5, 10, and 20 μg per defect, equivalent to 25, 50, and 100 μL, respectively. The graft materials were gently mixed and left at room temperature for approximately 30 minutes before implantation. All preparation procedures were performed under aseptic conditions. Throughout the study period, the animals were housed in stainless-steel cages under controlled environmental conditions, including a temperature of 19–21 °C, relative humidity of 45 ± 10%, and a 12-hour light/dark cycle. All animals were provided with a standard laboratory pellet diet and had free access to drinking water ad libitum. (11-13).

2.2. Surgical Protocol

All surgical interventions were performed under strict aseptic conditions. Anesthesia was induced by intramuscular injection of ketamine hydrochloride (35 mg/kg) and xylazine (5 mg/kg), as shown in Figure 1A. The calvarial region was then shaved and disinfected with povidone-iodine solution. A midline scalp incision was made, and a full-thickness flap was elevated to expose the calvarial bone. Four standardized full-thickness circular defects, each 5 mm in diameter, were created bilaterally in the parietal bones using a trephine bur under continuous sterile saline irrigation, as shown in Figure 1B. Care was taken to avoid injury to the sagittal suture and underlying dura mater (14).

The defects were treated according to the study design illustrated in Figure 2. The flap was then repositioned and sutured in layers. Postoperative care included intramuscular penicillin (100 mg/kg) once daily for three days and ketorolac tromethamine for analgesia for three days. All animals were monitored daily after surgery.

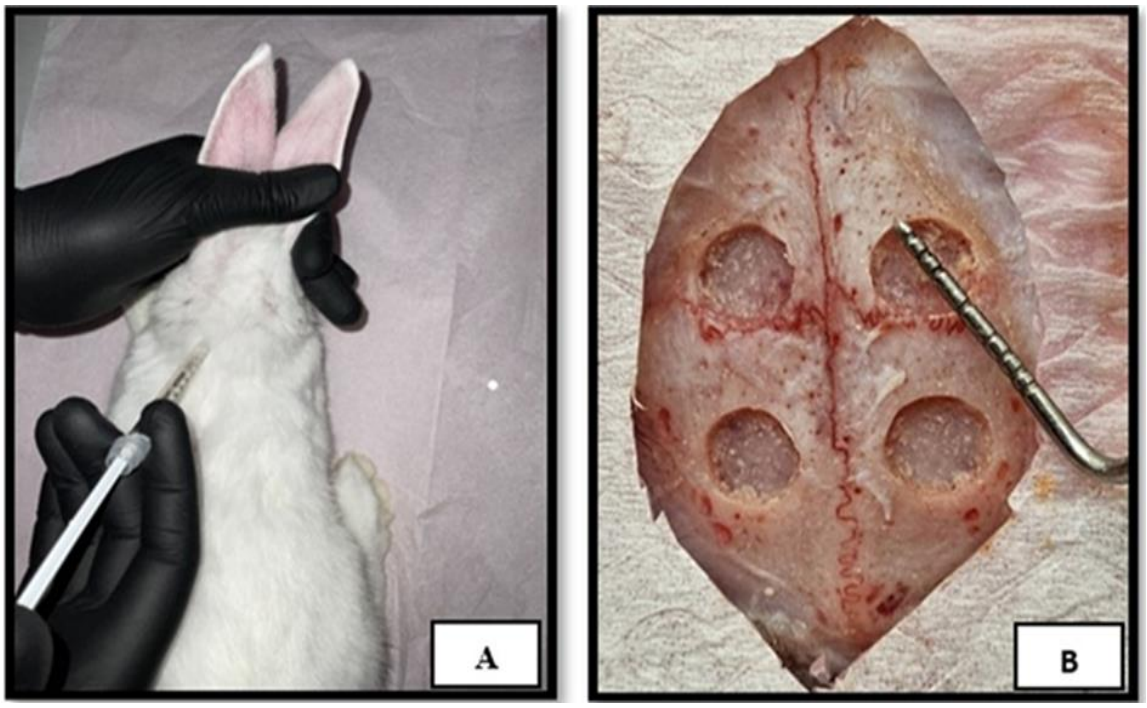

Figure 1. (A) Intramuscular anesthesia. (B) Creation and measurement of calvarial defects.

 doi:10.20944/preprints202603.1773.v1

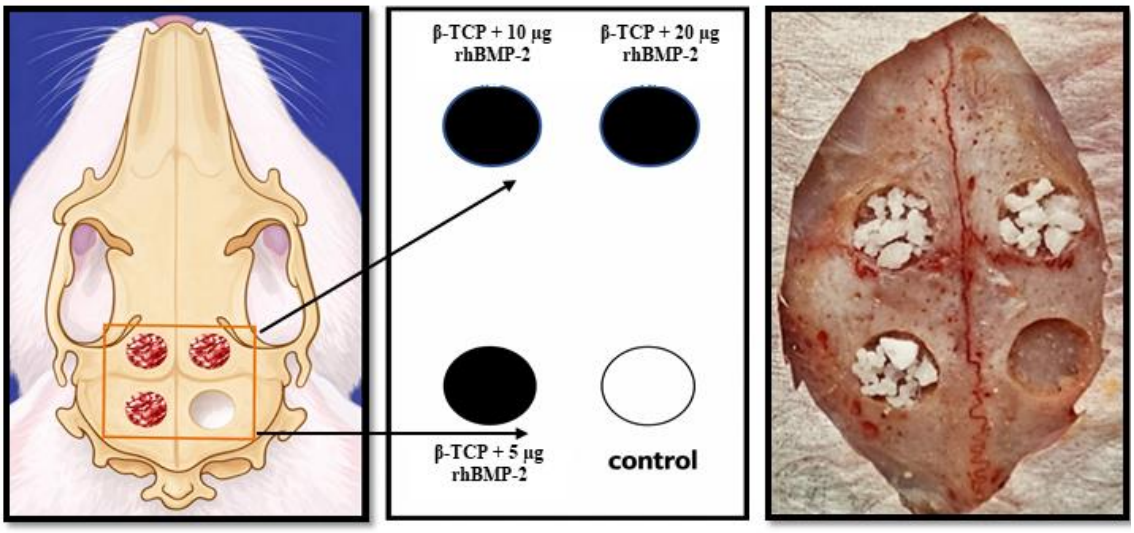

Figure 2. Schematic representation of β-TCP loaded with different doses of BMP-2 applied in 5-mm rabbit calvarial defects.

2.3. Histological Evaluation of Rabbit Calvarial Bone Defect

Animals were humanely euthanized at 2, 4, and 8 weeks after surgery, and the calvarial bone specimens were carefully harvested using a dental diamond disc. The samples were fixed in 10% neutral buffered formalin for 48–72 hours and subsequently decalcified in 10% formic acid for approximately 2–3 days. Following decalcification, the specimens were dehydrated through graded ethanol solutions, cleared in xylene, and embedded in paraffin wax for histological processing.

Serial sections approximately 5 μm thick were obtained through the center of each defect using a rotary microtome (Leica RM2135) (15, 16). The central sections from each block were selected for staining. The sections were stained with hematoxylin and eosin (H&E) for general histological evaluation and Masson's trichrome for the assessment of collagen deposition and maturation.

Histological evaluation of the stained sections was performed using a light microscope at ×400 magnification. Digital images were captured for qualitative and quantitative analysis of bone formation and tissue organization. The numbers of osteoblasts, osteocytes, and osteoclasts were counted in six randomly selected high-power fields (HPFs). To minimize observer bias, all histopathological assessments were conducted by an experienced histopathologist who was blinded to the experimental groups (17).

2.4. Histomorphometric Assessment

Quantitative histomorphometric evaluation of bone regeneration within the defect area was performed using a digital light microscope at ×400 magnification integrated with an image analysis system (Motic, ToupTek, ToupView (×86), version 3.7.4183, 2014). Digital images of microscopic fields covering the entire defect region were captured for analysis.

For quantitative assessment, the region of interest (ROI) was defined as the original defect area corresponding to the 5-mm circular calvarial defect created during surgery. The boundaries of the defect were identified histologically based on the margins of the native cortical bone surrounding the defect.

New bone formation within the ROI was identified according to its histological characteristics and measured using image analysis software. The area of newly formed bone was calculated and expressed as a percentage of the total defect area within the ROI.

Granulation tissue within the defect region was identified based on its histological appearance and evaluated semi-quantitatively using a histological scoring system. The inflammatory response was assessed by counting inflammatory cells, including neutrophils, lymphocytes, and macrophages.

 doi:10.20944/preprints202603.1773.v1

Each microscopic field was superimposed with a standardized 16-square grid to facilitate uniform and reproducible cell counting.

2.5. Evaluation of Inflammatory Reaction

The severity of the inflammatory response was determined based on the number of inflammatory cells observed at ×400 magnification in all experimental groups (18). The inflammatory cells were identified according to their morphological characteristics. The inflammatory reaction was graded according to the following criteria:

Score 0: Absence or presence of very few inflammatory cells (0–5), indicating no detectable inflammatory reaction.

Score 1: Between 5 and <25 cells, representing a mild inflammatory reaction.

Score 2: Between 25 and <125 cells, corresponding to a moderate inflammatory reaction.

Score 3: 125 cells or more, indicating a severe inflammatory reaction.

In addition to inflammatory cell counts, the presence of granulation tissue, degree of angiogenesis, and extent of fibrous tissue deposition were evaluated semi-quantitatively using a scoring system (19).

Score 0: Weak or minimal expression of the parameter.

Score 1: Moderate expression of the parameter.

Score 2: Strong or intense expression of the parameter.

2.6. Special Stains

Perls' Prussian blue stain was employed to identify iron deposition within the bone trabeculae. In addition, Masson's trichrome staining was used to evaluate the distribution and organization of collagen fibers. The extent and pattern of collagen maturation and arrangement were assessed semi-quantitatively according to the following criteria (20):

Score 0: Predominance of immature, thin collagen fibers arranged in a loose or reticular pattern.

Score 1: Moderate development of collagen fibers forming partially organized bundles.

Score 2: Abundant mature collagen fibers showing compact and parallel organization.

2.7. Immunohistochemical Analysis

Formalin-fixed, paraffin-embedded tissue sections (4-5µm thick) were subjected to immunohistochemical staining for CD31 to evaluate endothelial cell expression and vascularization within the regenerated tissue. The sections were deparaffinized in xylene and rehydrated through graded alcohols, followed by rinsing in distilled water. Heat-induced antigen retrieval was performed using EnVision FLEX Target Retrieval Solution in a PT Link instrument at 97 °C. After washing with EnVision FLEX Wash Buffer, the sections were incubated with a mouse monoclonal anti-CD31 antibody (clone JC70A, Dako/Agilent, Denmark) at room temperature. Subsequently, an HRP-conjugated secondary antibody from the EnVision FLEX detection system was applied according to the manufacturer's instructions. The antigen–antibody complexes were visualized using 3,3′-diaminobenzidine (DAB) as the chromogen, producing a brown reaction product at sites of CD31 expression. Finally, the sections were counterstained with hematoxylin, dehydrated through graded alcohols, cleared in xylene, and mounted with coverslips for microscopic examination.

The Immunostained slides were analyzed using ImageJ software (version 1.47v; National Institutes of Health, Bethesda, MD, USA). A standardized intensity threshold method was applied to identify CD31-positive areas, and the percentage of brown-stained regions was calculated for each specimen. The obtained data were subsequently subjected to statistical analysis to compare vascularization among the experimental groups (21).

 doi:10.20944/preprints202603.1773.v1

2.8. Statistical Analysis

Data are presented as mean ± standard deviation (SD). The normality of the data distribution was assessed using the Shapiro–Wilk test. For normally distributed data, differences between treatment groups and healing periods were analyzed using two-way analysis of variance (ANOVA) followed by Tukey's post hoc test for multiple comparisons. For non-parametric or ordinal data, the Kruskal–Wallis test followed by Dunn's post hoc test was applied. A p- value < 0.05 was considered statistically significant. All statistical analyses were performed using GraphPad Prism software. Sample sizes were determined by performing a power analysis using G*Power software based on new bone formation measurements obtained from previous studies using rabbit calvarial bone defect models. The statistical parameters were set at a power of 80% (1–β = 0.80) and a significance level of α = 0.05, with an estimated effect size of 0.40 derived from previously reported experimental data. These power calculations, together with previously reported data from similar calvarial defect experiments, suggested that a sample size of 5–6 animals per time point would be sufficient to detect statistically significant differences between experimental groups

3. Results

3.1. Histological Assessment of Calvarial Bone Defects (H&E, ×400)

Figure 3 shows the histological features of bone regeneration in the experimental groups at different healing intervals. In week two, the control group demonstrated predominantly immature tissue with inflammatory cell infiltration within the defect area. The β-TCP + 5 μg rhBMP-2 group showed fibrous connective tissue occupying the defect region with reduced inflammatory infiltration. In the β-TCP + 10 μg rhBMP-2 group, early bone matrix containing osteocyte lacunae was detected. The β-TCP + 20 μg rhBMP-2 group exhibited early new bone formation surrounded by bone matrix.

In week four, the control group showed fibrous connective tissue with limited bone matrix formation. The β-TCP + 5 μg rhBMP-2 group demonstrated bone matrix containing osteocytes within the defect area. The β-TCP + 10 μg rhBMP-2 group showed a thicker and more continuous bone matrix with visible vascular structures. In **the** β-TCP + 20 μg rhBMP-2 group, new bone formation with improved tissue organization was observed.

In week eight, the control group showed incomplete healing with persistent fibrous tissue and limited bone matrix formation. The β-TCP + 5 μg rhBMP-2 group demonstrated new bone formation within the defect area. Both the β-TCP + 10 μg rhBMP-2 and β-TCP + 20 μg rhBMP-2 groups exhibited mature bone formation characterized by organized bone matrix and numerous osteocyte lacunae, with the 20 μg rhBMP-2 group showing the most developed and well-organized bone architecture.

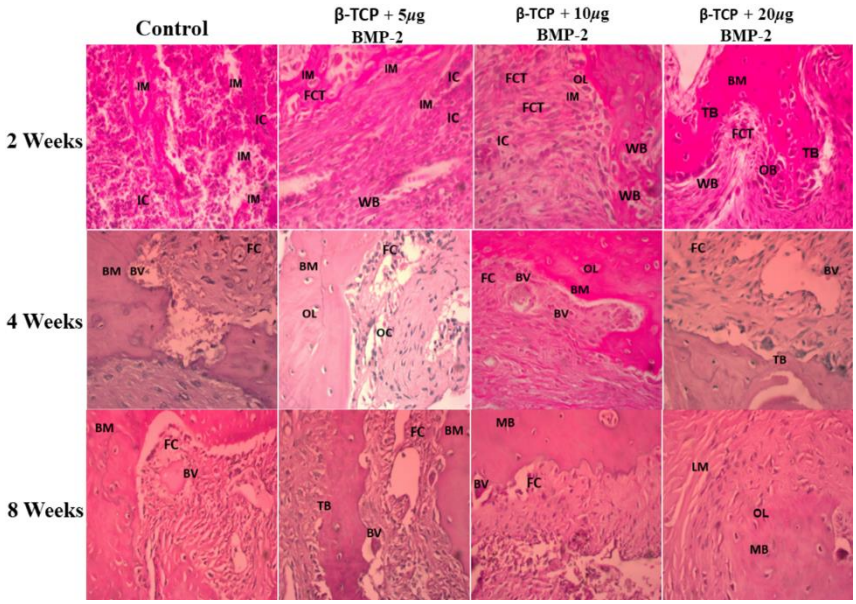

 doi:10.20944/preprints202603.1773.v1

Figure 3. Histological evaluation of rabbit calvarial defects treated with β-TCP loaded with different doses of rhBMP-2 at 2, 4, and 8 weeks. I; immature bone; IC, inflammatory cells; FC, fibrous connective tissue; BM, bone matrix; MB, mature bone; TB, trabecular bone; BV, blood vessel; OC, osteocyte; OL, Osteocyte Lacunae; LM, lamellar bone.

3.2. Histomorphometric Analysis of Bone Regeneration

3.2.1. New Bone Formation (%)

Quantitative histomorphometric analysis demonstrated a progressive increase in new bone formation across all groups during the healing period (Table 1; Figure 4). The amount of newly formed bone was greater in the rhBMP-2–treated groups compared with the control group and increased with higher rhBMP-2 doses.

In week two, the control group manifested the lowest level of bone formation (12.4 ± 3.1%). In contrast, the experimental groups treated with β-TCP loaded with rhBMP-2 showed higher values. The β-TCP + 5 μg rhBMP-2 group demonstrated 18.6 ± 3.8%, while the β-TCP + 10 μg rhBMP-2 group reached 22.9 ± 4.0%, and the β-TCP + 20 μg rhBMP-2 group showed the highest bone formation at this time point (27.3 ± 4.4%).

In week four, a marked increase in bone regeneration was observed in all groups. The control group showed 25.7 ± 4.2% new bone formation. Higher values were observed in the β-TCP + 5 μg rhBMP-2 group (36.2 ± 4.5%), followed by the β-TCP + 10 μg rhBMP-2 group (45.1 ± 5.2%), while the β-TCP + 20 μg rhBMP-2 group exhibited the greatest bone formation (50.6 ± 5.9%).

In week eight, bone regeneration further increased across all groups. The control group reached 38.5 ± 5.0%, whereas the β-TCP + 5 μg rhBMP-2 group showed 52.4 ± 6.1%. The β-TCP + 10 μg rhBMP-2 group demonstrated 65.8 ± 6.7%, while the β-TCP + 20 μg rhBMP-2 group displayed the highest value of new bone formation (72.9 ± 7.2%).

Table 1. Quantitative Analysis of new bone formation (%) in Control and β-TCP Loaded with Different Doses of BMP-2 in week 2, 4, and 8 (Mean ± SD).

Groups	Week two New bone formation (%)	week four New bone formation (%)	8 Weeks New bone formation (%)
Control	12.4 ± 3.1	25.7 ± 4.2	38.5 ± 5.0
β-TCP +5μg rhBMP-2	18.6 ± 3.8*	36.2 ± 4.5*	52.4 ± 6.1*
β-TCP+10 μg rhBMP-2	22.9 ± 4.0**	45.1 ± 5.2**	65.8 ± 6.7**
β-TCP+20 μgrhBMP-2	27.3 ± 4.4***	50.6 ± 5.9***	72.9 ± 7.2***

*p < 0.05, ** p < 0.01, *** p < 0.001.

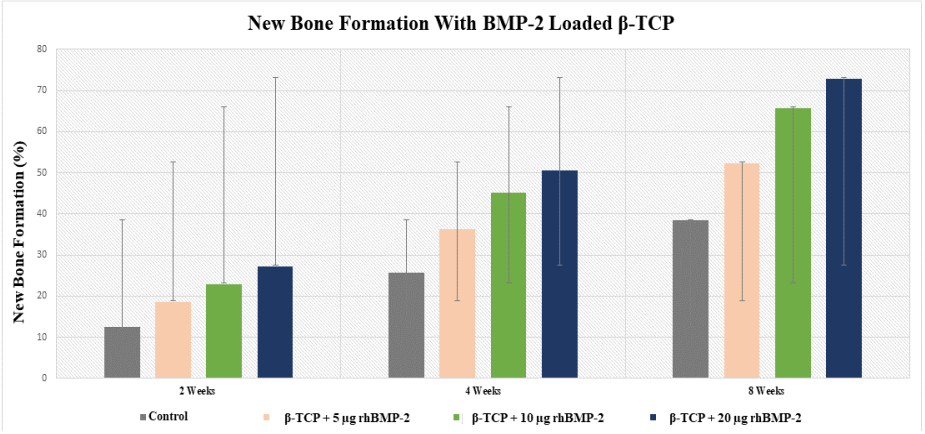

 doi:10.20944/preprints202603.1773.v1

Figure 4. New bone formation (%) in rabbit calvarial defects treated with β-TCP loaded with different doses of BMP-2 at 2, 4, and 8 weeks. Data are presented as mean ± SD.

3.2.2. Inflammatory Response and Granulation Tissue

In week two, the control group indicated the highest inflammatory reaction (2.33 ± 0.52), whereas rhBMP-2-treated groups presented lower mean scores that decreased progressively with increasing rhBMP-2 dosage ,1.67 ± 0.52 for (β-TCP + 5 µg rhBMP-2) 1.33 ± 0.52 for (β-TCP + 10 µg rhBMP-2), and 1.00 ± 0.00 for (β-TCP + 20 µg rhBMP-2). Granulation tissue formation was absent in the control group (0.00 ± 0.00) but evident in the BMP-2-treated groups, with mild to moderate fibro-angiogenic tissue particularly in the (β-TCP + 5 µg rhBMP-2) group (1.33 ± 0.52) as illustrated in (Figure 5 a-b).

In week four, inflammatory scores declined across all groups, reaching 1.25 ± 0.50 in the control group and stabilizing at 1.00 ± 0.00 in the rhBMP-2-treated groups. Granulation tissue scores remained mild and consistent among rhBMP-2 groups (1.00 ± 0.00), while the control group exhibited slightly higher values (1.33 ± 0.52) as illustrated in (Figure 5 a-b).

In week eight, inflammatory activity was minimal in all groups, with complete absence in the (β-TCP + 10 µg rhBMP-2 and β-TCP + 20 µg rhBMP-2) groups (0.00 ± 0.00). Granulation tissue formation showed a further reduction, with mean scores of 1.33 ± 0.52 in the control group, 1.00 ± 0.00 in the (β-TCP+5µg rhBMP-2) group, 0.33 ± 0.52 in the (β-TCP+10 µg rhBMP-2) group, and 0.00 ± 0.00 in the (β-TCP+20 µg rhBMP-2) group, as illustrated in (Figure 5 a-b).

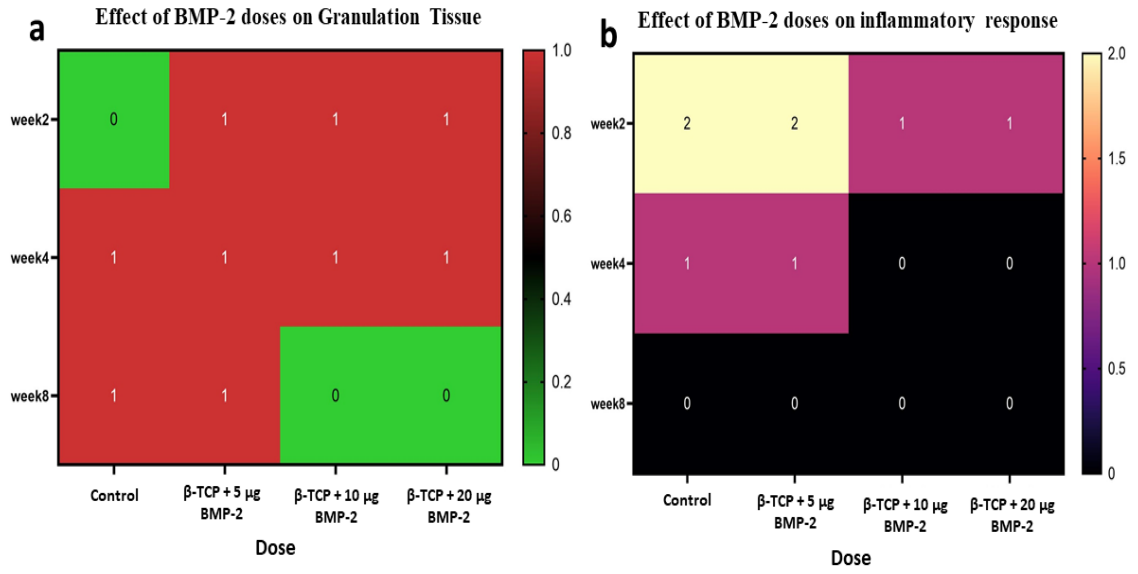

Figure 5. Heatmap analysis of granulation tissue formation (a) and inflammatory response (b) in rabbit calvarial defects treated with different doses of BMP-2.

3.3. Quantitative Analysis of Bone Cell Counts

The mean (± SD) numbers of osteocytes, osteoblasts, and osteoclasts varied among groups across the healing intervals, with similar values observed between 4 and 8 weeks in several groups.

Osteocytes: In the control group, osteocyte counts increased significantly from week two to week four and eight ($p < 0.0001$), while the difference between week four and eight was not statistically significant. In the β-TCP + 5 µg rhBMP-2 group, osteocyte numbers increased significantly, in week four compared with week two ($p < 0.0001$) and decreased in week eight, although the values remained significantly higher than those in week two ($p < 0.0001$). In the β-TCP + 10 µg rhBMP-2 and β-TCP + 20 µg rhBMP-2 groups, osteocyte counts were highest in week two and decreased significantly at 4 and 8 weeks ($p < 0.001$), with no significant difference between 4 and 8 weeks (Figure 6a).

 doi:10.20944/preprints202603.1773.v1

Osteoblasts: In the control group, osteoblast counts increased significantly from week two to week four ($p < 0.0001$) and further increased in week eight ($p < 0.0001$). In the β-TCP + 5 µg rhBMP-2 group, osteoblast numbers increased significantly in week four compared with week two ($p < 0.0001$) and decreased in week eight, although remaining significantly higher than those in week two ($p < 0.0001$). In the β-TCP + 10 µg rhBMP-2 and β-TCP + 20 µg rhBMP-2 groups, osteoblast counts were highest in week two and decreased significantly at 4 and 8 weeks ($p < 0.0001$) (Figure 6b).

Osteoclasts: In the control group, osteoclast counts remained low in week two, four and eight with no statistically significant differences. In the β-TCP + 5 µg rhBMP-2 group, osteoclast numbers increased significantly in week four compared with week two ($p < 0.0001$) and remained similar in week eight. In the β-TCP + 10 µg rhBMP-2 and β-TCP + 20 µg rhBMP-2 groups, osteoclast counts increased significantly in week four and eight compared with week two ($p < 0.0001$), with no significant difference between 4 and 8 weeks (Figure 6c)

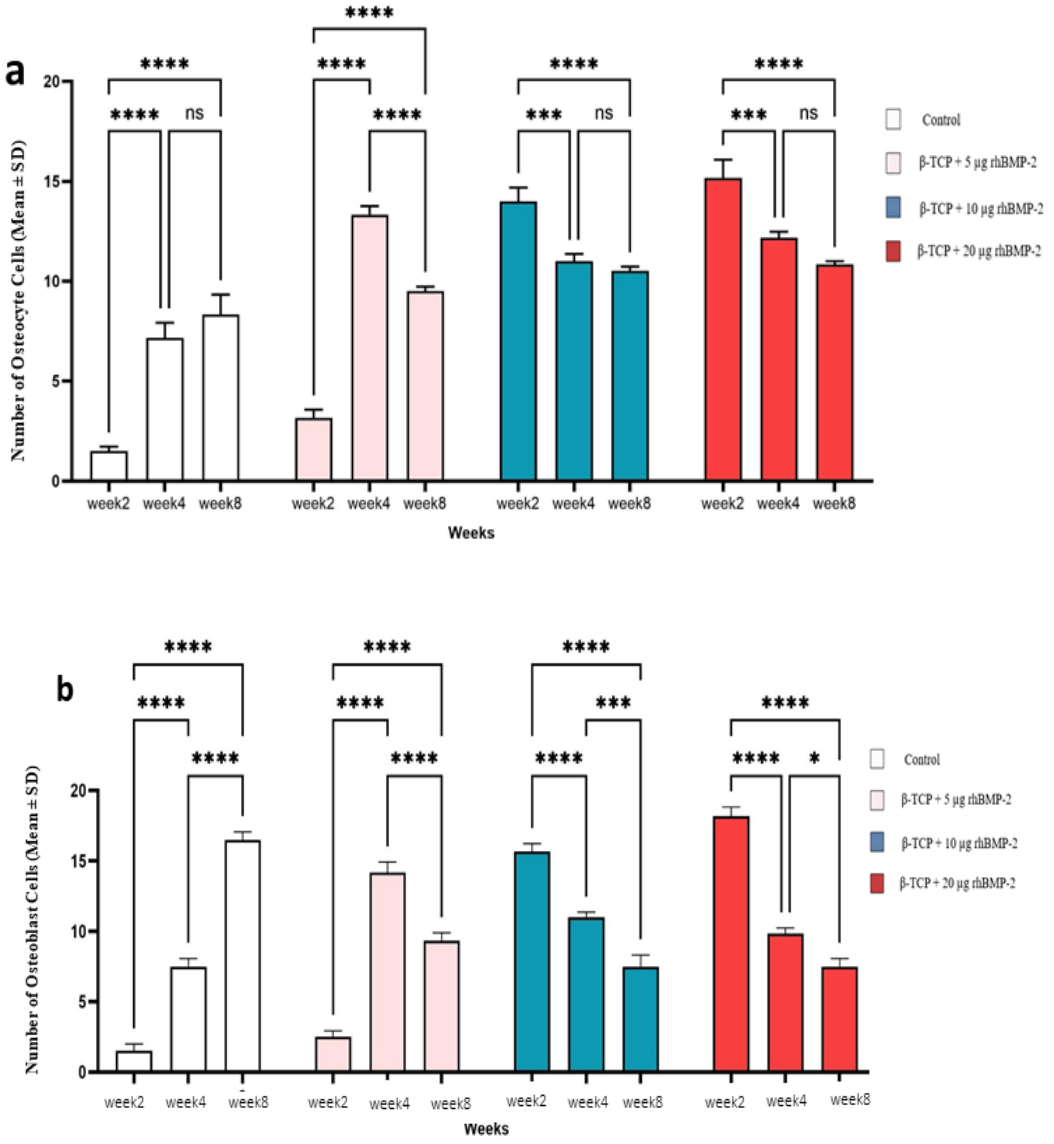

 doi:10.20944/preprints202603.1773.v1

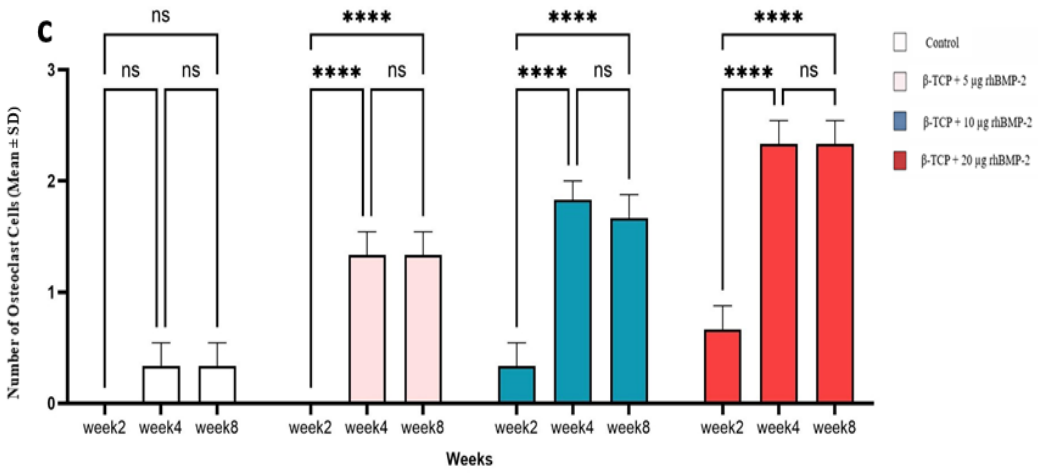

Figure 6. Quantitative analysis of bone cell populations during healing of rabbit calvarial defects treated with different doses of rhBMP-2 loaded β-TCP scaffolds (a) Number of osteocyte cells (mean ± SD), (b) number of osteoblast cells (mean ± SD), and (c) number of osteoclast cells (mean ± SD) in the defect sites in week two, four and eight postoperatively. Four experimental groups were evaluated: control, β-TCP + 5µg rhBMP-2, β-TCP + 10µg rhBMP-2, and, β-TCP + 20µg rhBMP-2. Bars represent mean values with standard deviation. Statistical significance between groups and time points is indicated as follows: *p < 0.05, **p < 0.01, ***p < 0.001, ****p < 0.0001; ns indicates non-significant differences.

3.4. Special Stains – Masson's Trichrome

Masson's trichrome staining demonstrated progressive collagen deposition and matrix maturation in all experimental groups during the healing period (Figure 7a–b).

In week two, the control group predominantly showed immature collagen fibers arranged in a loose reticular pattern (Score 0) with minimal new bone formation. In contrast, the β-TCP + 5 µg rhBMP-2 group exhibited moderately organized collagen fibers (Score 1) accompanied by early vascular structures and initial new bone formation. The β-TCP + 10 µg rhBMP-2 and β-TCP + 20 µg rhBMP-2 groups also demonstrated moderately organized collagen fibers (Score 1) with increased vascularization and more evident new bone formation.

In week four, the control group presented moderately organized collagen bundles (Score 1) with limited new bone formation. The β-TCP + 5 µg rhBMP-2 group showed similar collagen organization with increased vascularization. In contrast, the β-TCP + 10 µg rhBMP-2 and β-TCP + 20 µg rhBMP-2 groups displayed dense and more organized collagen bundles (Score 2) associated with increased new bone formation and vascular structures.

In week eight, the control group continued to show moderately organized collagen fibers (Score 1). In comparison, all rhBMP-2–treated groups demonstrated dense, mature collagen bundles (Score 2) together with well-developed new bone and prominent vascular structures. The β-TCP + 20 µg rhBMP-2 group exhibited the most advanced collagen organization and bone formation.

 doi:10.20944/preprints202603.1773.v1

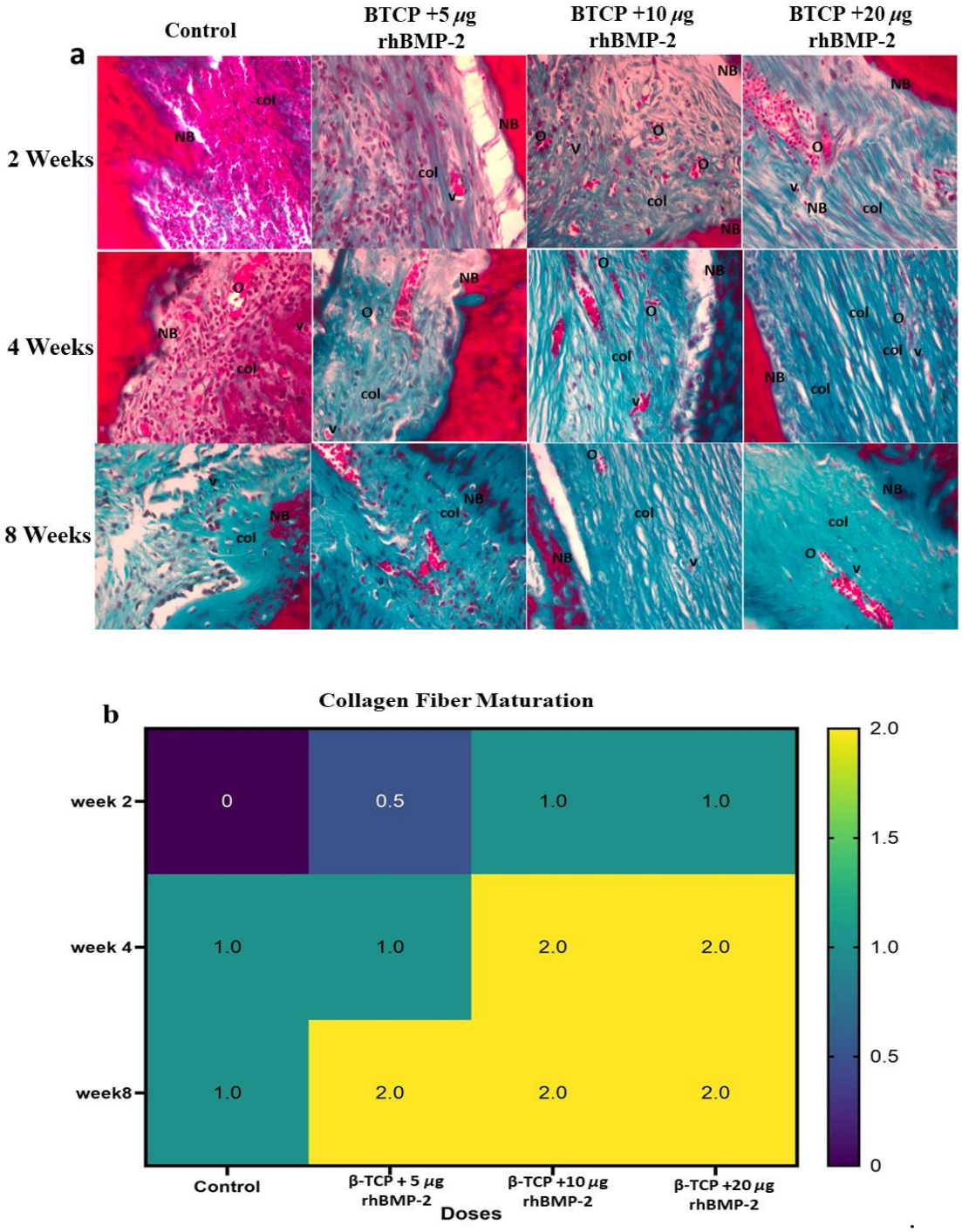

Figure 7. (a) Representative Masson's trichrome–stained histological sections showing collagen fiber deposition and maturation during bone healing in the control and BMP-2–treated groups at different healing periods. (b) Corresponding heatmap analysis illustrating the semi-quantitative scoring and distribution of collagen fiber maturation among the experimental groups. NB: new bone; col: collagen fibers; V: blood vessel; O: osteon.

3.5. CD31 Immunohistochemical Analysis

Representative CD31 immunohistochemical staining demonstrated differences in vascular expression among the experimental groups during the healing period (Figure 8), and these findings were supported by quantitative analysis of the CD31-positive vascular area (%) (Table 2). In week two, the control defects exhibited weak CD31-positive staining with a mean vascular area of 10.2 ± 2.1%. In contrast, the β-TCP + rhBMP-2 groups showed stronger CD31 immunoreactivity, with mean values of 19.6 ± 3.2% in the β-TCP + 5 μg rhBMP-2 group, 26.8 ± 3.7% in the β-TCP + 10 μg rhBMP-2 group, and 31.4 ± 4.0% in the β-TCP + 20 μg rhBMP-2 group.

 doi:10.20944/preprints202603.1773.v1

In week four, CD31 expression increased in the control group (18.5 ± 3.4%), while the β-TCP + 5 μg rhBMP-2, β-TCP + 10 μg rhBMP-2, and β-TCP + 20 μg rhBMP-2 groups showed mean vascular areas of 17.4 ± 2.9%, 21.2 ± 3.1%, and 23.5 ± 3.3%, respectively.

In week eight, CD31-positive staining decreased in all groups compared with earlier intervals. The control group presented a mean vascular area of 12.3 ± 2.8%, whereas the β-TCP + 5 μg rhBMP-2, β-TCP + 10 μg rhBMP-2, and β-TCP + 20 μg rhBMP-2 groups demonstrated 11.5 ± 2.4%, 13.1 ± 2.5%, and 14.2 ± 2.7%, respectively.

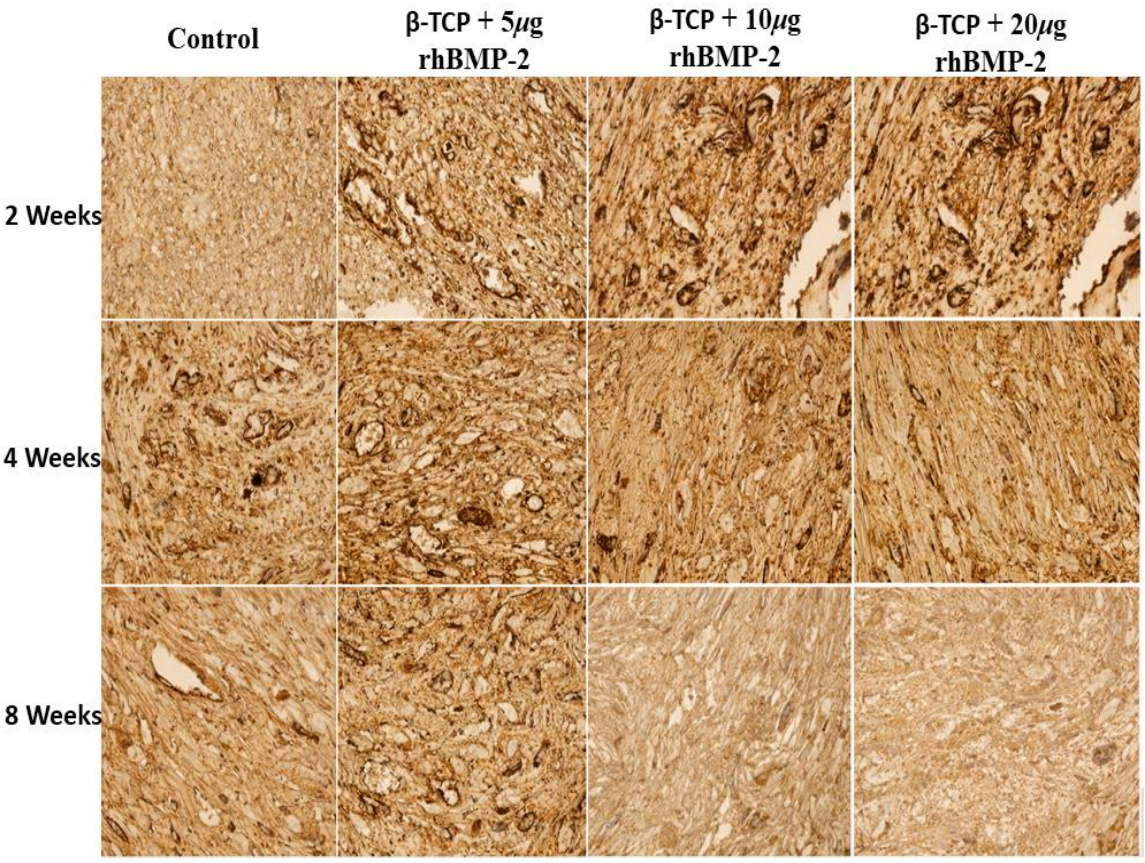

Figure 8. Representative CD31 immunohistochemical staining illustrating blood vessel formation and angiogenesis in the control and β-TCP + rhBMP-2–treated groups at different healing periods (2, 4, and 8 weeks).

Table 2. Quantitative analysis of CD31-positive vascular area (%) in rabbit calvarial defects treated with β-TCP loaded with different doses of rhBMP-2 at different healing periods.

Groups	Week two (Mean ± SD %)	Week four (Mean ± SD %)	Week eight (Mean ± SD %)
Control	10.2 ± 2.1	18.5 ± 3.4	12.3 ± 2.8
β-TCP + 5 μg rhBMP-2	19.6 ± 3.2*	17.4 ± 2.9 ns	11.5 ± 2.4 ns
β-TCP + 10 μg rhBMP-2	26.8 ± 3.7***	21.2 ± 3.1**	13.1 ± 2.5*
β-TCP + 20 μg rhBMP-2	31.4 ± 4.0***	23.5 ± 3.3**	14.2 ± 2.7*

* $p < 0.05$, ** $p < 0.01$*** $p < 0.001$.

4. Discussion

Bone morphogenetic protein-2 (BMP-2) is widely recognized as one of the most potent osteoinductive growth factors involved in bone regeneration. It has been extensively investigated in bone tissue engineering because of its ability to stimulate osteoblast differentiation, extracellular matrix production, and new bone formation (22). However, previous experimental and clinical

 doi:10.20944/preprints202603.1773.v1

studies have reported that excessively high rhBMP-2 doses may lead to adverse effects such as soft-tissue swelling, inflammatory reactions, and ectopic bone formation. These findings highlight the importance of determining an optimal and safe dosage for clinical applications (13, 23).

The rabbit calvarial model is commonly used in experimental bone regeneration studies because it is surgically accessible, provides a stable cortical surface, and allows reliable evaluation of biomaterials and osteogenic growth factors (22). In such models, critical-size defects (CSDs) are created to properly evaluate regenerative materials. These defects are defined as bone defects that do not heal spontaneously during the lifetime of the animal without intervention (13, 24).

In rabbit calvarial models, circular defects ranging from 5–8 mm are commonly used to evaluate bone healing (25). In the present study, 5-mm calvarial defects were selected because they allow reliable assessment of bone regeneration while maintaining structural stability of the calvarial bone. Therefore, this study investigated the regenerative potential of three rhBMP-2 doses (5 μg, 10 μg, and 20 μg) delivered through β-TCP scaffolds to determine the most effective dose for enhancing bone regeneration in calvarial defects.

Histopathological evaluation demonstrated clear differences in bone regeneration between the control and rhBMP-2–treated groups. The control defects showed limited osteoid deposition and minimal new bone formation, with most of the defect space occupied by fibrovascular connective tissue. This pattern reflects the delayed and incomplete spontaneous healing typically observed in critical-size bone defects in the absence of osteoinductive stimuli or grafting materials (26, 27).

In contrast, defects treated with rhBMP-2 exhibited clear signs of active osteogenesis, including early osteoid deposition, alignment of osteoblast-like cells along the margins of the defect, and progressive new bone formation. With increasing healing time, these regenerative features became more evident, particularly in the β-TCP + 20 μg rhBMP-2 group, where the defect was largely bridged by continuous mineralized new bone containing numerous osteocytes within lacunae by eight weeks. Although the β-TCP + 10 μg and β-TCP + 5 μg rhBMP-2 groups also demonstrated evident bone repair, the degree of bone organization and mineralization was comparatively less pronounced. These observations suggest that rhBMP-2 enhances osteogenic differentiation and matrix deposition, while the β-TCP scaffold provides an osteoconductive framework that supports cell attachment and bone ingrowth. Similar findings have been reported in studies demonstrating that rhBMP-2 delivered through calcium-phosphate biomaterials accelerates bone formation and improves the structural organization of regenerated bone tissue (28-30).

Quantitative analysis of new bone formation further supported the histological observations. At the early two-week interval, the control group exhibited minimal new bone formation, indicating limited spontaneous healing of the defect. In contrast, all rhBMP-2–treated groups demonstrated substantially greater bone formation. These findings are consistent with previous studies reporting that osteoinductive growth factors can significantly accelerate early bone regeneration when combined with osteoconductive scaffolds (27, 31).

As healing progressed to four and eight weeks, the area of newly formed bone increased in all groups, reflecting continued bone deposition and maturation. Higher rhBMP-2 doses maintained the greatest bone formation values throughout the healing period. However, the difference between the 10 μg and 20 μg rhBMP-2 groups was not statistically significant at later intervals. This observation suggests that increasing the rhBMP-2 dose beyond a certain threshold may not produce proportional increases in new bone formation, which is consistent with studies describing a plateau effect during later stages of bone healing.

The inflammatory response and granulation tissue formation observed in this study demonstrated clear time- and dose-related changes following rhBMP-2 application. At the early stage of healing, the control defects exhibited the most pronounced inflammatory reaction, whereas the rhBMP-2–treated groups showed noticeably milder inflammatory activity. This pattern suggests that rhBMP-2 may help moderate the early inflammatory phase of bone repair and contribute to the establishment of a more favorable microenvironment for tissue regeneration (32). In contrast to the control defects, granulation tissue formation was evident in the rhBMP-2–treated groups, particularly

 doi:10.20944/preprints202603.1773.v1

in the lower-dose group. The presence of fibro-angiogenic granulation tissue reflects early fibroblast proliferation and neovascularization, which are characteristic features of the initial reparative phase of bone healing (33).

As healing progressed, inflammatory activity gradually declined in all experimental groups, indicating the normal transition from the inflammatory phase to the proliferative stage of tissue repair. During this stage, granulation tissue remained present in the rhBMP-2–treated defects but appeared more organized and structured. This organization likely reflects ongoing vascular maturation and connective tissue remodeling, which are essential for supporting subsequent bone formation. Previous studies have reported that BMP-2 signaling may influence inflammatory pathways and improve healing conditions by promoting angiogenesis and regulating cellular responses within the defect site (34, 35).

With further progression of healing, inflammatory cells became largely absent in the higher-dose rhBMP-2 groups, and granulation tissue formation was markedly reduced. These changes indicate the transition from the proliferative phase to the remodeling stage of bone repair. The gradual resolution of inflammation together with the reduction of granulation tissue suggests that rhBMP-2 may facilitate the progression of healing toward tissue remodeling and bone maturation while maintaining the normal sequence of the regenerative process. Similar observations have been reported in previous studies, which demonstrated that BMP-2 can accelerate the progression of bone healing by promoting the transition from early inflammatory and proliferative phases toward advanced remodeling and bone maturation (34, 36).

The cellular responses observed in this study further highlight the osteogenic activity of rhBMP-2. All rhBMP-2–treated groups exhibited higher numbers of osteoblasts and osteocytes compared with the control group, indicating enhanced osteogenic activity and accelerated maturation of regenerated bone tissue. These findings are consistent with studies demonstrating that BMP-2 promotes the recruitment and differentiation of mesenchymal progenitor cells into osteoblasts through activation of Smad signaling pathways and up-regulation of key osteogenic transcription factors such as RUNX2 and Osterix (34, 36, 37). Osteoclasts were also observed in the BMP-2 groups, particularly at later healing intervals, indicating active bone remodeling. Osteoclast-mediated resorption plays an essential role in the transition of newly formed woven bone into mature lamellar bone (36). Recent studies suggest that BMP-2 regulates both osteoblast differentiation and osteoclast activity, thereby coordinating the balance between bone formation and resorption during bone regeneration (38-41). This coordinated cellular activity contributes to the development of structurally organized and mechanically functional bone tissue.

Masson's trichrome staining further demonstrated a clear dose-dependent progression of collagen deposition and extracellular matrix maturation during the healing process. Collagen fibers gradually increased in density and organization from week two to week eight in all experimental groups; however, the rhBMP-2–treated defects showed more pronounced collagen deposition and improved fiber alignment compared with the control group. Early healing stages in the control defects were characterized by loosely arranged and immature collagen fibers, whereas BMP-2–treated groups already exhibited moderate collagen deposition and partial bundle organization. As healing progressed, collagen bundles became progressively thicker and more organized, particularly in the β-TCP + 10 μg rhBMP-2 and β-TCP + 20 μg rhBMP-2 groups. These findings indicate that BMP-2 enhances extracellular matrix maturation and promotes earlier structural organization of the regenerating bone matrix. This effect may be attributed to the osteoinductive activity of rhBMP-2, which stimulates osteogenic differentiation and type I collagen synthesis, while β-TCP provides an osteoconductive scaffold that facilitates cell attachment and extracellular matrix deposition within the defect site (42, 43). Previous studies have similarly reported that BMP-2 accelerates collagen matrix formation and promotes maturation of regenerated bone tissue in experimental models of bone repair (43-45).

Immunohistochemical analysis of CD31 demonstrated increased vascular expression in BMP-2–treated defects compared with the control group. During the early healing stage (week two), BMP-2–

 doi:10.20944/preprints202603.1773.v1

treated groups showed markedly stronger CD31 staining, indicating enhanced vascularization within the defect area. The β-TCP + 10 μg rhBMP-2 and β-TCP + 20 μg rhBMP-2 groups exhibited the highest vascular areas at this stage, suggesting that rhBMP-2 stimulated early angiogenic activity during bone healing. Similar findings have been reported in previous experimental studies demonstrating that rhBMP-2 enhances early vascularization and promotes the formation of new blood vessels during bone regeneration (35, 46).

In week four, vascularization increased in the control group and remained elevated in the higher-dose rhBMP-2 groups, whereas a slight decrease in vascular area was observed in the β-TCP + 5 μg rhBMP-2 group. This transient reduction may reflect early maturation and stabilization of the vascular network rather than reduced angiogenesis. Previous studies have indicated that vascular remodeling commonly occurs during intermediate healing stages as immature capillary networks become organized and stabilized within the regenerating tissue (33, 46).

In week eight, CD31 expression decreased in all groups compared with earlier healing intervals. This reduction likely reflects the transition from the early angiogenic phase toward tissue maturation and bone remodeling, during which newly formed blood vessels become stabilized and less numerous. Similar temporal patterns of vascular regression during late bone healing stages have been described in experimental models of bone regeneration (33, 39).

Angiogenesis plays a critical role in bone regeneration because newly formed blood vessels supply oxygen, nutrients, and osteogenic cells to the regenerating tissue. Previous studies have shown that BMP-2 can indirectly promote angiogenesis by stimulating osteogenic cells to release vascular endothelial growth factor (VEGF) and other angiogenic mediators (46, 47).

Taken together, the histological, histomorphometric, and CD31 immunohistochemical findings of the present study demonstrate that rhBMP-2–loaded β-TCP scaffolds enhance bone regeneration in critical-size defects. Regenerative outcomes improved with increasing BMP-2 dosage, with the β-TCP + 20 μg rhBMP-2 group showing the most pronounced regenerative response. These findings support the interaction between osteogenesis and angiogenesis during bone healing and support the role of rhBMP-2 in promoting both processes when delivered through an osteoconductive scaffold system. Future studies should incorporate three-dimensional imaging techniques such as micro-computed tomography (micro-CT) to provide a more comprehensive evaluation of bone volume and architecture. In addition, the use of additional immunohistochemical markers may help to further elucidate the mechanisms of osteogenesis and angiogenesis. Studies with longer healing periods are also recommended to assess the long-term maturation and stability of the regenerated bone.

5. Conclusion

Loading of rhBMP-2 into β-tricalcium phosphate scaffolds markedly promoted bone regeneration in rabbit critical-sized calvarial defects, showing a clear dose-dependent enhancement in bone healing. As the healing period progressed, defects treated with rhBMP-2 demonstrated gradual and continuous improvements, beginning with early osteoid deposition and advancing toward more mature, well-organized bone. Among the tested concentrations, the (β-TCP + 20 μg rhBMP-2) formulation produced the most pronounced osteoinductive activity at all time points, characterized by extensive new bone formation, enhanced collagen maturation, and well-developed vascularization. These findings suggest that rhBMP-2 loaded β-TCP scaffolds may represent a promising strategy for enhancing bone regeneration in craniofacial bone defects and may have potential applications in oral and maxillofacial reconstructive procedures.

Author Contributions: Conceptualization, S.A.M.; methodology, S.A.M.; validation, R.A.A.; formal analysis, S.A.M.; investigation, S.A.M.; data curation, S.A.M.; writing—original draft preparation, S.A.M.; writing—review and editing, C.A.M. and R.A.A.; visualization, S.A.M.; supervision, C.A.M.; histological and histomorphometric analysis, R.A.A. All authors have read and agreed to the published version of the manuscript.

Funding: This research received no external funding.

 doi:10.20944/preprints202603.1773.v1

Institutional Review Board Statement: The animal study protocol was approved by the Animal Ethics Committee of Hawler Medical University, Erbil, Iraq (Approval No.: HMUD-2425061, approved on 22 December 2024). All procedures were conducted in accordance with the ARRIVE (Animal Research: Reporting of In Vivo Experiments) guidelines and institutional regulations for animal care and use.

Informed Consent Statement: Not applicable.

Data Availability Statement: The datasets generated and analyzed during the current study, including histological images and histomorphometric measurements, are available from the corresponding author upon reasonable request.

Acknowledgments: The authors would like to express their sincere appreciation to the staff of the animal research facility and the laboratory team at Hawler Medical University for their technical assistance and support during the experimental procedures and histological preparations. The authors also acknowledge the valuable guidance and support provided throughout the course of this research. During the preparation of this manuscript, the authors used ChatGPT (OpenAI, GPT-5) for language editing and assistance in improving the clarity of the manuscript. The authors reviewed and edited the generated content and take full responsibility for the final content of this publication.

Conflicts of Interest: The authors declare no conflict of interest.

Abbreviations

The following abbreviations are used in this manuscript:

Abbreviation	Definition
BMP-2	Bone Morphogenetic Protein-2
rhBMP-2	Recombinant Human Bone Morphogenetic Protein-2
β-TCP	Beta-tricalcium phosphate
CSD/CSDs	Critical-size defect/critical-size defects
H&E	Hematoxylin and eosin
HPF/HPFs	High-power field/high-power fields
ROI	Region of interest
SD	Standard deviation
ANOVA	Analysis of variance
HRP	Horseradish peroxidase
DAB	3,3′-Diaminobenzidine
RANKL	Receptor activator of nuclear factor kappa-B ligand
TGF-β	Transforming growth factor beta
VEGF	Vascular endothelial growth factor
RUNX2	Runt-related transcription factor 2

References

1. Uribe F, Vásquez B, Alister JP, Olate S. Comparison of rhBMP-2 in Combination with Different Biomaterials for Regeneration in Rat Calvaria Critical-Size Defects. BioMed Research International. 2022;2022(1):6281641.
2. Uribe F, Vasquez B, Veuthey C, Alister JP, Olate S. Influence of rhBMP-2 on bone repair of critical size defects with different biomaterials. International Journal of Morphology. 2020;38(2):316-21.
3. Velásquez H, Olate S, Díaz C, Navarro P, Borie E, de Moraes M. Quantitation of mandibular symphysis bone as source of bone grafting: description in class I and class III skeletal conditions. Journal of Oral Implantology. 2017;43(3):211-7.
4. Diaz-Rodriguez P, Sánchez M, Landin M. Drug-loaded biomimetic ceramics for tissue engineering. Pharmaceutics. 2018;10(4):272.
5. Wei L, Yu D, Wang M, Deng L, Wu G, Liu Y. Dose effects of slow-released bone morphogenetic protein-2 functionalized β-tricalcium phosphate in repairing critical-sized bone defects. Tissue Engineering Part A. 2020;26(3-4):120-9.

 doi:10.20944/preprints202603.1773.v1

6. Miron RJ, Sculean A, Shuang Y, Bosshardt DD, Gruber R, Buser D, et al. Osteoinductive potential of a novel biphasic calcium phosphate bone graft in comparison with autographs, xenografts, and DFDBA. Clinical oral implants research. 2016;27(6):668-75.
7. Urist MR. Bone: formation by autoinduction. Science. 1965;150(3698):893-9.
8. Arias-Betancur A, Badilla-Wenzel N, Astete-Sanhueza Á, Farfán-Beltrán N, Dias FJ. Carrier systems for bone morphogenetic proteins: An overview of biomaterials used for dentoalveolar and maxillofacial bone regeneration. Japanese Dental Science Review. 2022;58:316-27.
9. El Bialy I, Jiskoot W, Reza Nejadnik M. Formulation, delivery and stability of bone morphogenetic proteins for effective bone regeneration. Pharmaceutical research. 2017;34:1152-70.
10. Kamal AF, Siahaan OSH, Fiolin J. Various dosages of BMP-2 for management of massive bone defect in Sprague Dawley rat. Archives of Bone and Joint Surgery. 2019;7(6):498.
11. Bien ND, Miura K-i, Sumita Y, Nakatani Y, Shido R, Kajii F, et al. Bone regeneration by low-dose recombinant human bone morphogenetic protein-2 carried on octacalcium phosphate collagen composite. Journal of Hard Tissue Biology. 2020;29(2):123-30.
12. Jung N, Park J, Park S-H, Oh S, Kim S, Cho S-W, et al. Improving bone formation by guided bone regeneration using a collagen membrane with rhBMP-2: a novel concept. Journal of Functional Biomaterials. 2023;14(3):170.
13. Choi JW, Jeong WS, Yang SJ, Park EJ, Oh TS, Koh KS. Appropriate and effective dosage of BMP-2 for the ideal regeneration of calvarial bone defects in beagles. Plastic and reconstructive surgery. 2016;138(1):64e-72e.
14. Schlund M, Depeyre A, Ranganath SK, Marchandise P, Ferri J, Chai F. Rabbit calvarial and mandibular critical-sized bone defects as an experimental model for the evaluation of craniofacial bone tissue regeneration. Journal of stomatology, oral and maxillofacial surgery. 2022;123(6):601-9.
15. Miquelestorena-Standley E, Jourdan M-L, Collin C, Bouvier C, Larousserie F, Aubert S, et al. Effect of decalcification protocols on immunohistochemistry and molecular analyses of bone samples. Modern Pathology. 2020;33(8):1505-17.
16. Fadhil E, Dosh RH, Wally ZJ, Haider J. Histological evaluation of the effects of bone morphogenetic protein 9 and angiopoietin 1 on bone healing. Journal of Taibah University Medical Sciences. 2023;18(5):954-63.
17. Savi FM, Brierly GI, Baldwin J, Theodoropoulos C, Woodruff MA. Comparison of different decalcification methods using rat mandibles as a model. Journal of Histochemistry & Cytochemistry. 2017;65(12):705-22.
18. Edwards III DF, Miller CJ, Quintana Martinez A, Wright CS, Prideaux M, Atkins GJ, et al. Differential iron requirements for osteoblast and adipocyte differentiation. Journal of Bone and Mineral Research Plus. 2021;5(9):e10529.
19. Mitic A, Todorovic K, Stojiljkovic N, Stojanovic N, Ilic S, Todorovic A, et al. Beneficial effects of curcumin on the wound-healing process after tooth extraction. Natural Product Communications. 2017;12(12):1934578X1701201223.
20. Chakraborty S, Tewari S, Sharma RK, Narula SC, Ghalaut PS, Ghalaut V. Impact of iron deficiency anemia on chronic periodontitis and superoxide dismutase activity: a cross-sectional study. Journal of periodontal & implant science. 2014;44(2):57-64.
21. Sharef AY, Hamdi BA, Alrawi RA, Ahmad HO. Onopordum acanthium L. extract attenuates pancreatic β-Cells and cardiac inflammation in streptozocin-induced diabetic rats. Plos one. 2023;18(1):e0280464.
22. Lee J-W, Lim H-C, Lee E-U, Park J-Y, Lee J-S, Lee D-W, et al. Paracrine effect of the bone morphogeneticprotein-2 at the experimental site on healing of the adjacent control site: a study in the rabbit calvarial defect model. Journal of Periodontal & Implant Science. 2014;44(4):178-83.
23. Lee KB, Taghavi CE, Murray SS, Song KJ, Keorochana G, Wang JC. BMP induced inflammation: a comparison of rhBMP-7 and rhBMP-2. Journal of Orthopaedic Research. 2012;30(12):1985-94.
24. Hassanein AH, Couto RA, Kurek KC, Rogers GF, Mulliken JB, Greene AK. Experimental comparison of cranial particulate bone graft, rhBMP-2, and split cranial bone graft for inlay cranioplasty. The Cleft Palate-Craniofacial Journal. 2013;50(3):358-62.
25. Tannoury CA, An HS. Complications with the use of bone morphogenetic protein 2 (BMP-2) in spine surgery. The Spine Journal. 2014;14(3):552-9.

 doi:10.20944/preprints202603.1773.v1

26. Li G, Shen W, Tang X, Mo G, Yao L, Wang J. Combined use of calcium phosphate cement, mesenchymal stem cells and platelet-rich plasma for bone regeneration in critical-size defect of the femoral condyle in mini-pigs. Regenerative Medicine. 2021;16(5):451-64.
27. Ni X, Feng J, Liang M, Zhou F, Xia Y, Dong Z, et al. Enhancing Bone Repair with β-TCP-Based Composite Scaffolds: A Review of Design Strategies and Biological Mechanisms. Orthopedic Research and Reviews. 2025:313-40.
28. Chung C-H, Kim Y-K, Lee J-S, Jung U-W, Pang E-K, Choi S-H. Rapid bone regeneration by Escherichia coli-derived recombinant human bone morphogenetic protein-2 loaded on a hydroxyapatite carrier in the rabbit calvarial defect model. Biomaterials research. 2015;19(1):17.
29. Kim J, Lee S, Choi Y, Choi J, Kang B-J. Sustained release of bone morphogenetic protein-2 through alginate microbeads enhances bone regeneration in rabbit tibial metaphyseal defect model. Materials. 2021;14(10):2600.
30. Li L, Yang L, Yang Y, Zhu J, Shi R, Deng Q, et al. 3D printed scaffolds loaded with BMP-2 for bone defect regeneration: a systematic review and meta-analysis. Frontiers in Physiology. 2025;16:1641937.
31. Zhao L, Zhao X, Deng F, Ye X, Shen Z, Xia Y, et al. Integration of BMP-2/PLGA microspheres with the 3D printed PLGA/CaSO4 scaffold enhances bone regeneration. Frontiers in Materials. 2024;11:1374409.
32. Fan Q, Bai J, Shan H, Fei Z, Chen H, Xu J, et al. Implantable blood clot loaded with BMP-2 for regulation of osteoimmunology and enhancement of bone repair. Bioactive Materials. 2021;6(11):4014-26.
33. Marsell R, Einhorn TA. The biology of fracture healing. Injury. 2011;42(6):551-5.
34. Wang J, Xue Y, Wang Y, Liu C, Hu S, Zhao H, et al. BMP-2 functional polypeptides relieve osteolysis via bi-regulating bone formation and resorption coupled with macrophage polarization. NPJ Regenerative medicine. 2023;8(1):6.
35. Çakır-Özkan N, Eğri S, Bekar E, Altunkaynak BZ, Kabak YB, Kıvrak EG. The use of sequential VEGF-and BMP2-releasing biodegradable scaffolds in rabbit mandibular defects. Journal of Oral and Maxillofacial Surgery. 2017;75(1):221. e1-. e14.
36. Zou M-L, Chen Z-H, Teng Y-Y, Liu S-Y, Jia Y, Zhang K-W, et al. The Smad dependent TGF-β and BMP signaling pathway in bone remodeling and therapies. Frontiers in molecular biosciences. 2021;8:593310.
37. Ingwersen L-C, Frank M, Naujokat H, Loger K, Bader R, Jonitz-Heincke A. BMP-2 long-term stimulation of human pre-osteoblasts induces osteogenic differentiation and promotes transdifferentiation and bone remodeling processes. International Journal of Molecular Sciences. 2022;23(6):3077.
38. Zhang L, Jiao G, Ren S, Zhang X, Li C, Wu W, et al. Exosomes from bone marrow mesenchymal stem cells enhance fracture healing through the promotion of osteogenesis and angiogenesis in a rat model of nonunion. Stem cell research & therapy. 2020;11(1):38.
39. Bahney CS, Zondervan RL, Allison P, Theologis A, Ashley JW, Ahn J, et al. Cellular biology of fracture healing. Journal of Orthopaedic Research®. 2019;37(1):35-50.
40. Heubel B, Nohe A. The role of BMP signaling in osteoclast regulation. Journal of developmental biology. 2021;9(3):24.
41. Shen H, Zhuang Y, Zhang C, Zhang C, Yuan Y, Yu H, et al. Osteoclast-driven osteogenesis, bone remodeling and biomaterial resorption: a new profile of BMP2-CPC-induced alveolar bone regeneration. International journal of molecular sciences. 2022;23(20):12204.
42. Carreira A, Lojudice FH, Halcsik E, Navarro R, Sogayar MC, Granjeiro JM. Bone morphogenetic proteins: facts, challenges, and future perspectives. Journal of dental research. 2014;93(4):335-45.
43. Bohner M, Santoni BLG, Döbelin N. β-tricalcium phosphate for bone substitution: Synthesis and properties. Acta biomaterialia. 2020;113:23-41.
44. Park H, Collignon A-M, Lepry WC, Ramirez-GarciaLuna JL, Rosenzweig DH, Chaussain C, et al. Acellular dense collagen-S53P4 bioactive glass hybrid gel scaffolds form more bone than stem cell delivered constructs. Materials Science and Engineering: C. 2021;120:111743.
45. Wang G, Roohani-Esfahani S-I, Zhang W, Lv K, Yang G, Ding X, et al. Effects of Sr-HT-Gahnite on osteogenesis and angiogenesis by adipose derived stem cells for critical-sized calvarial defect repair. Scientific reports. 2017;7(1):41135.

 doi:10.20944/preprints202603.1773.v1

46. Kim J-H, Kim C-J, Shin S-H. Bone Healing in Ovariectomized-rabbit Calvarial Defect with Tricalcium Phosphate Coated with Recombinant Human Bone Morphogenetic Protein-2 Genetically Engineered in Escherichia coli. Maxillofacial Plastic and Reconstructive Surgery. 2014;36(2):37.
47. Lee DK, Ki M-R, Kim EH, Park C-J, Ryu JJ, Jang HS, et al. Biosilicated collagen/β-tricalcium phosphate composites as a BMP-2-delivering bone-graft substitute for accelerated craniofacial bone regeneration. Biomaterials research. 2021;25(1):13.